JBC RESEARCH ARTICLE

Regulation of cell size and Wee1 kinase by elevated levels of the cell cycle regulatory protein kinase Cdr2

Received for publication, November 7, 2022, and in revised form, December 12, 2022 Published, Papers in Press, December 24, 2022,
https://doi.org/10.1016/j.jbc.2022.102831

Rachel A. Berg and James B. Moseley*

From the Department of Biochemistry and Cell Biology, The Geisel School of Medicine at Dartmouth, Hanover, New Hampshire, USA

Edited by Henrik Dohlman

Many cell cycle regulatory proteins catalyze cell cycle progression in a concentration-dependent manner. In the fission yeast *Schizosaccharomyces pombe*, the protein kinase Cdr2 promotes mitotic entry by organizing cortical oligomeric nodes that lead to inhibition of Wee1, which itself inhibits the cyclin-dependent kinase Cdk1. *cdr2Δ* cells lack nodes and divide at increased size due to overactive Wee1, but it has not been known how increased Cdr2 levels might impact Wee1 and cell size. It also has not been clear if and how Cdr2 might regulate Wee1 in the absence of the related kinase Cdr1/Nim1. Using a tetracycline-inducible expression system, we found that a 6× increase in Cdr2 expression caused hyperphosphorylation of Wee1 and reduction in cell size even in the absence of Cdr1/Nim1. This overexpressed Cdr2 formed clusters that sequestered Wee1 adjacent to the nuclear envelope. Cdr2 mutants that disrupt either kinase activity or clustering ability failed to sequester Wee1 and to reduce cell size. We propose that Cdr2 acts as a dosage-dependent regulator of cell size by sequestering its substrate Wee1 in cytoplasmic clusters, away from Cdk1 in the nucleus. This mechanism has implications for other clustered kinases, which may act similarly by sequestering substrates.

The core elements of the eukaryotic cell cycle include a regulatory network that promotes switch-like entry into mitosis at the G2/M transition. Activated cyclin-dependent kinase Cdk1 bound to its cyclin subunit phosphorylates diverse substrates to drive mitotic entry (1, 2). In G2, the Cdk1-cyclin complex is kept inactive by Wee1 kinase, which inhibits Cdk1 by phosphorylating a conserved tyrosine residue (3, 4). At the G2/M transition, Cdk1 inhibition is reversed by the phosphatase Cdc25, which removes the inhibitory tyrosine phosphorylation from Cdk1 (3, 5). Activated Cdk1-cyclin then inhibits Wee1 and activates Cdc25, resulting in dual feedback loops for switch-like mitotic entry (2). In the fission yeast *Schizosaccharomyces pombe*, a long-standing model organism for cell cycle research, regulation of these conserved cell cycle proteins establishes cell size at division. More specifically, fission yeast cells enter mitosis at a reproducible size due to size-dependent activation of Cdk1 regulated in part by Wee1 and Cdc25 (6).

Many of these proteins act as dosage-dependent regulators of fission yeast cell size at division, consistent with their known activities and mechanisms. For example, loss-of-function mutations in *wee1+* cause cells to divide at a small size due to over-active Cdk1, while *wee1+* overexpression increases cell size at division (7). Conversely, mutations in *cdc25+* increase cell size, while *cdc25+* overexpression reduces cell size (8). Wee1 activity in cells is regulated in a size-dependent manner by the protein kinases Cdr1 and Cdr2 (9), which are conserved SAD family kinases. Cdr1 (also called Nim1) directly phosphorylates Wee1 to inhibit its kinase activity (10–13). Cdr1 acts in a dosage-dependent manner: loss-of-function causes elongated cells due to over-active Wee1, while *cdr1+* overexpression reduces cell size at division (14). These results are consistent with Cdc25, Wee1, and Cdr1 acting as concentration-dependent catalytic regulators of their substrates.

Cdr2 also promotes Wee1 inhibition in cells but does not appear to inhibit Wee1 kinase activity directly (15). Rather, Cdr2 forms oligomeric "nodes" at the plasma membrane and recruits both Cdr1 and Wee1 to these structures (9, 16–18). Consistent with this mechanism, loss-of-function mutations in *cdr2+* increase cell size (15, 19, 20). Our work in this study addresses two open questions regarding Cdr2, a central regulator of cell size. First, it has been unclear if and how Cdr2 acts on cell size in a dosage-dependent manner. Strong *cdr2+* overexpression with the $P3_{nmt1}$ promoter is lethal, and cells exhibit pleiotropic defects including multiseptation and branching (20). $P3_{nmt1}$-*cdr2+* overexpression causes a shift in the migration of Wee1 by Western blot (13), but the lethality of this strong overexpression system prevented further mechanistic and functional studies. Lower levels of *cdr2+* overexpression with the weakened $P81_{nmt1}$ reduce cell size (21, 22), but the underlying mechanism has not been studied.

A second open question addressed in our work is whether Cdr2 regulates Wee1 and cell size independently of Cdr1/Nim1. Recent work has led to the model that Cdr2 nodes act as scaffolds to promote inhibitory phosphorylation of Wee1 by Cdr1 (9, 13). In this model, the function of Cdr2 on Wee1 and cell size requires Cdr1. However, it has long been noted that *cdr2Δ* mutants have a more severe cell size defect than *cdr1Δ*

* For correspondence: James B. Moseley, james.b.moseley@dartmouth.edu.

mutants (17–19), suggesting additional roles beyond promoting inhibitory phosphorylation. One possibility is that Cdr2 spatially sequesters Wee1 away from the nucleus, which separates Wee1 from its nuclear target Cdk1. However, this possibility has not been tested with orthogonal approaches to loss-of-function mutations in Cdr2. Spatial regulation of Wee1 by Cdr2 in combination with catalytic inhibition by Cdr1 would provide a robust, two-pronged mechanism for cell size control. Such spatial mechanisms have been observed in other kinase signaling pathways (23–26) as well as for Cdc25 (27), the protein phosphatase that counteracts Wee1 activity on Cdk1 and cell size.

Here, we increased *cdr2+* expression with a tetracycline-regulated promoter recently adapted for controlled expression in *S. pombe* (28). We discovered that increased expression of *cdr2+* induces Wee1 hyperphosphorylation and sequestration at cytoplasmic clusters, leading to premature mitotic entry and reduced cell size at division. These findings establish Cdr2 as a dosage-dependent regulator of cell size through a localization-based mechanism.

Results

We used the tetracycline-induced expression system to control levels of Cdr2. In the presence of anhydrotetracycline (Tet), P_{Tet}-*GST-cdr2* (hereafter P_{Tet}-*cdr2*) integrated at the *leu1+* locus slowed the migration of Wee1-FLAG by SDS-PAGE, but catalytically inactive mutants P_{Tet}-*cdr2(E177A)* and P_{Tet}-*cdr2(T166A)* did not affect Wee1-FLAG (Figs. 1*A* and S1*A*). We confirmed that P_{Tet}-*cdr2* induced a similar shift for untagged Wee1 (Fig. S1*B*). This band shift was due to hyperphosphorylation because it was reversed by treatment with λ-phosphatase (Fig. 1*B*). To determine the level of overexpression responsible for this effect, we generated a P_{Tet}-*cdr2-5FLAG* construct for comparison with *cdr2-5FLAG* expressed by the endogenous promoter at the endogenous chromosomal locus. By quantitative Western blot of whole cell lysates, the level of P_{Tet}-*cdr2-5FLAG* was six times higher than endogenously expressed *cdr2-5FLAG* (Fig. 1*C*). We considered that hyperphosphorylation of Wee1 might involve the presence of endogenously expressed Cdr1 and Cdr2 in this system, so we repeated this experiment in *cdr1Δ cdr2Δ* cells. Interestingly, P_{Tet}-*cdr2* still induced hyperphosphorylation of Wee1 in *cdr1Δ cdr2Δ* cells (Figs. 1*D* and S1*C*), showing that this modification is not mediated by Cdr1.

Next, we tested the effects of P_{Tet}-*cdr2* on cell size. Addition of Tet to P_{Tet}-*cdr2* cells caused a marked and significant decrease in cell length at division (Fig. 2, *A* and *B*). In contrast, Tet-based overexpression of *cdr2(E177A)* increased the size of dividing cells, consistent with dominant-negative effects for

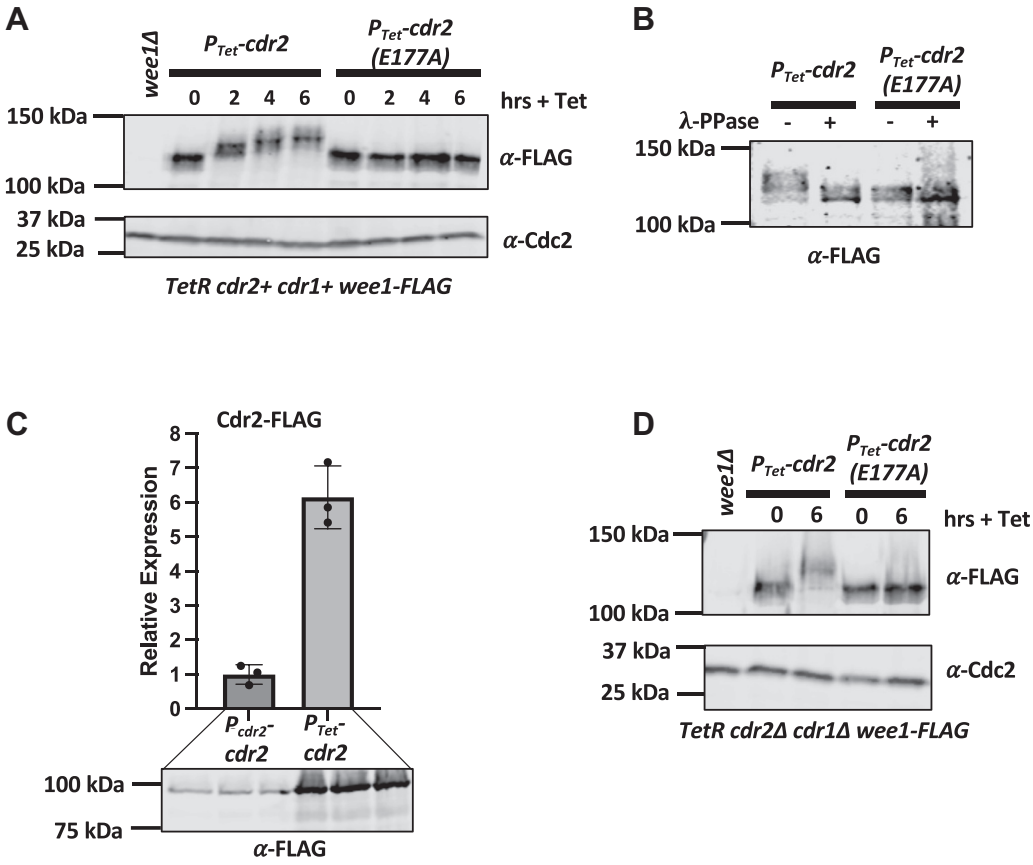

Figure 1. Tet-regulated Cdr2 overexpression induces hyperphosphorylation of Wee1. *A*, whole-cell extracts were separated by SDS-PAGE and Western blotted to detect Wee1-FLAG after induction of wildtype Cdr2 or kinase-dead Cdr2(E177A). *B*, gel shift induced by Cdr2 overexpression is reversed by λ-phosphatase. *C*, Western blot quantification of cellular Cdr2-FLAG protein overexpression. Graph shows data points normalized to the average signal for P_{cdr2}-*cdr2-FLAG* samples. Error bars indicate standard deviation. See Experimental procedures for more details. *D*, hyperphosphorylation of Wee1 does not require endogenous Cdr1 or Cdr2. Cdc2 was probed as a loading control. Tet, anhydrotetracycline.

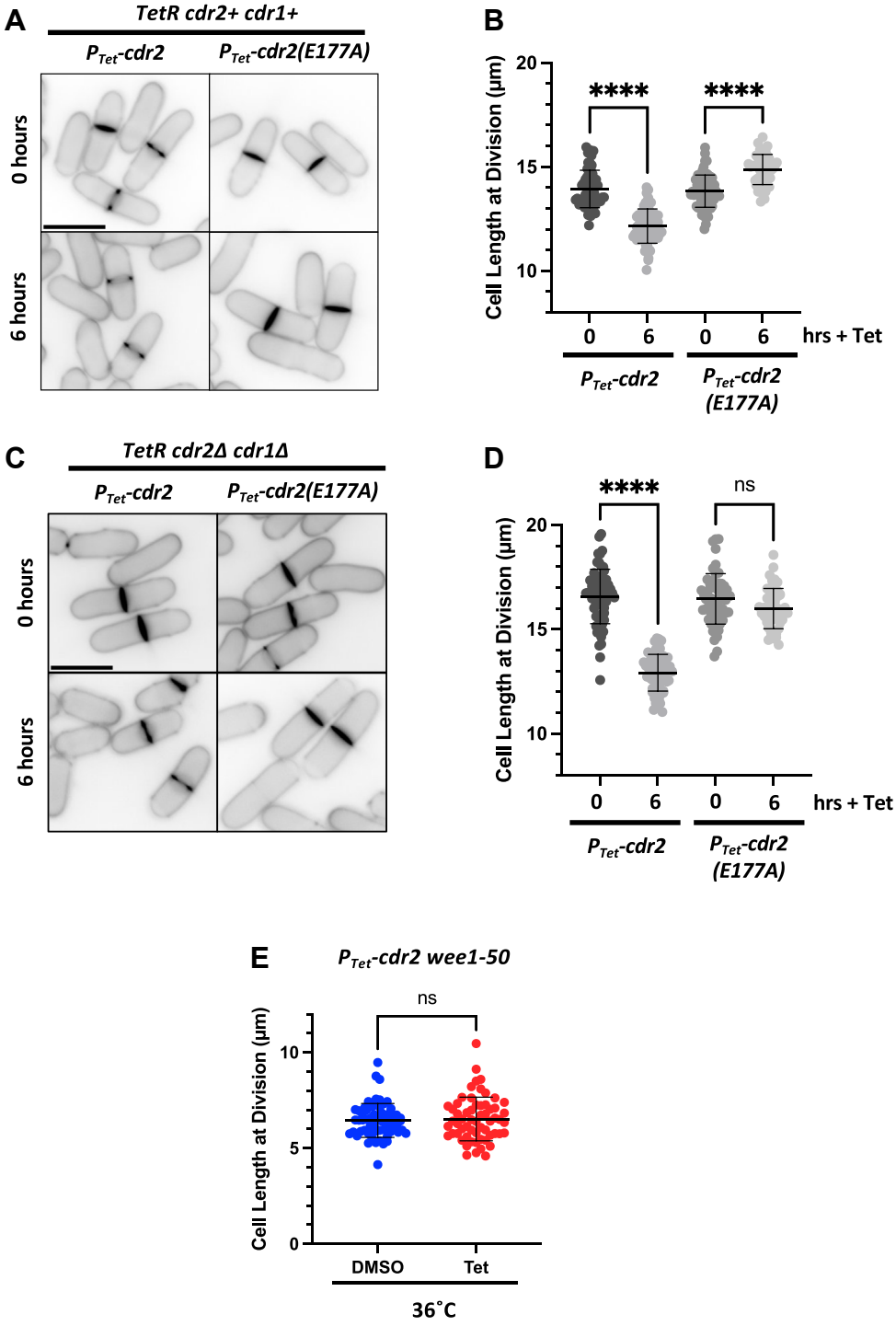

Figure 2. P_{Tet}-*cdr2* reduces cell size at division. *A*, Blankophor-stained images of cells before and after Tet treatment. Scale bar, 10 µm. *B*, cell length at division for the indicated strains and treatments. n ≥ 50 cells each. *C*, Blankophor-stained images of *cdr1Δ cdr2Δ* cells before and after Tet treatment. Scale bar, 10 µm. *D*, cell length at division for the indicated strains and treatments. n ≥ 50 cells each. *E*, cell length at division for P_{Tet}-*cdr2 wee1-50* cells grown at the nonpermissive temperature of 36 C for 4 h. ns, not significant ($p > 0.05$). ****$p < 0.0001$ determined by ANOVA (panels *B* and *D*) or Welch's *t* test (panel *E*). Tet, anhydrotetracycline.

this inactive mutant. Cdr2 controls cell size by recruiting Wee1 to cortical nodes where it is inhibited by Cdr1 (9, 13), so we considered that P_{Tet}-*cdr2* effects on cell size might require Cdr1. However, induction of P_{Tet}-*cdr2* in *cdr1Δ cdr2Δ* cells still reduced cell size, whereas P_{Tet}-*cdr2(E177A)* had no effect (Fig. 2, *C* and *D*). These results indicate that P_{Tet}-*cdr2* induces Wee1 hyperphosphorylation and reduces cell size by a mechanism that is independent of Cdr1.

We used genetic epistasis to investigate the underlying pathway. If P_{Tet}-*cdr2* regulates cell size through Wee1, then it should have no effect in the absence of Wee1 activity. Consistent with this prediction, P_{Tet}-*cdr2* did not reduce cell

size in the temperature-sensitive *wee1-50* mutant grown at 36 C (Fig. 2*E*). We conclude that increased levels of Cdr2 cause hyperphosphorylation of Wee1 leading to reduced cell size at division.

To determine the mechanism for P_{Tet}-*cdr2* regulation of Wee1, we examined the localization of mEGFP-Cdr2 induced by P_{Tet}. Previous studies have shown that Cdr2 exerts spatial control over the Wee1 regulatory pathway. In addition to cortical nodes along cell sides, which are seen for endogenously expressed mEGFP-Cdr2, we observed bright cytoplasmic puncta for both mEGFP-Cdr2 and mEGFP-Cdr2(E177A) expressed by the P_{Tet} promoter (Fig. 3*A*). Interestingly, induction of P_{Tet}-*cdr2* caused recruitment of Wee1-mNG to similar cytoplasmic clusters (Fig. 3*B*). This redistribution of Wee1 required Cdr2 kinase activity because it was lost in the P_{Tet}-*cdr2(E177A)* mutant (Fig. 3*B*).

Next, we performed a series of colocalization experiments on these P_{Tet}-*mEGFP-cdr2* cytoplasmic clusters. Upon induction, P_{Tet}-*mEGFP-cdr2* recruited endogenously expressed Cdr2-mCherry to cytoplasmic clusters (Fig. 3*C*), and this effect was independent of Cdr2 kinase activity (Fig. S2*A*). Using endogenously expressed Cdr2-mCherry as a marker for clusters, we found that Wee1-mNG and Cdr2-mCherry colocalized in the same cytoplasmic clusters when expression of P_{Tet}-*cdr2* was induced from the *leu1+* locus (Fig. 3*D*). In contrast, the inactive mutant P_{Tet}-*cdr2(E177A)* did not drive colocalization of Wee1-mNG and Cdr2(E177A)-mCherry at cytoplasmic clusters (Fig. S2*B*).

Together, our results show that both active Cdr2 and inactive Cdr2(E177A) localize to cytoplasmic clusters upon expression with P_{Tet}. However, only active Cdr2 clusters can recruit Wee1, induce Wee1 hyperphosphorylation, and reduce cell size at division. These results lead to a simple model in which Cdr2 clusters sequester Wee1 away from its nuclear target Cdk1, causing premature entry into mitosis.

Based on this working model, we sought additional information about these Cdr2 cytoplasmic clusters. Cdr2 recruits Cdr1 kinase, Arf6 GTPase, and anillin-like Mid1 to cortical nodes (17, 18, 29, 30). We did not observe strong recruitment of either Cdr1 or Arf6 to cytoplasmic clusters in P_{Tet}-*cdr2* cells (Fig. 4, *A* and *B*). However, Mid1 localized to cytoplasmic clusters in P_{Tet}-*cdr2* cells but not in P_{Tet}-*cdr2(E177A)* cells, where it localized in the typical distribution of the nucleus and cortical nodes (Fig. 4*C*). We conclude that Cdr2, Wee1, and Mid1 might be the primary components of these clusters, and Cdr2 kinase activity is required for recruitment of both Wee1 and Mid1 to these structures.

To probe the nature of Cdr2 interactions within clusters, we treated cells with 1,6-hexanediol, which disrupts weak, hydrophobic molecular interactions (31–33) and also can impair the activity of some protein kinases and phosphatases (34). Cdr2 cytoplasmic clusters disappeared after 10 min of treatment with 5% hexanediol (Fig. 5*A*). This result indicates that Cdr2 clusters are held together by weak interactions and are not irreversibly aggregated, although we cannot rule out contributions from 1,6-hexanediol effects on the activity of cellular kinases and phosphatases (34). Interestingly, endogenous Cdr2 nodes also were dispersed by the same 1,6-hexanediol treatment (Fig. 5*B*). This result suggests that Cdr2 cytoplasmic clusters and endogenous Cdr2 nodes are held together by similar biophysical properties.

mEGFP-Cdr2 clusters can be found throughout the cytoplasm, but we noted that Wee1-mNG clusters in P_{Tet}-*cdr2* cells are restricted to the cell middle and absent from cell ends. Using the ER marker Sur4-mCherry and the nuclear envelope marker Cut11-mCherry, we found that Wee1-mNG clusters in P_{Tet}-*cdr2* cells are restricted to the nuclear periphery and/or nuclear ER (Fig. 6, *A* and *B*). We considered the possibility that these clusters might be the spindle pole body, which is embedded in the nuclear envelope, but Wee1-mNG clusters did not colocalize with the spindle pole body marker Sad1-mCherry (Fig. 6*C*; no colocalization in 20 of 22 cells examined). These results show that Cdr2 clusters can be found throughout the cytoplasm, but only clusters associated with the nucleus can capture and sequester Wee1.

Finally, we used the P_{Tet} system to define the domains of Cdr2 required for cluster formation and effects on both Wee1 and cell size. The Cdr2 N terminus contains a kinase domain and a ubiquitin-associated domain, which is thought to be necessary for kinase activity (35) (Fig. 7*A*). The Cdr2 C terminus contains a KA1 domain (kinase associated-1) and a basic patch, both of which promote binding to membranes (36). Between the N terminus and C terminus is a linker domain that is predicted to be unstructured. Using P_{Tet} to drive expression, neither Cdr2(1–330) nor Cdr2(1–590) truncations reduced cell size or formed cytoplasmic clusters (Fig. 7, *B–D*) despite expression of all constructs to similar levels (Fig. S3*A*). In fact, expression of catalytically active versions of both truncations increased cell size (Fig. 7, *B* and *C*), demonstrating a dominant negative effect. This result suggests that clustering mediated by the KA1 domain is required for reduction of cell size, and expression of non-clustering mutants inhibits the endogenous cell size regulatory system. Interestingly, P_{Tet}-*cdr2(1–590)* was capable of inducing Wee1 hyperphosphorylation despite a lack of clustering. P_{Tet}-*cdr2(1–330)* did not induce Wee1 hyperphosphorylation, but stronger overexpression with the thiamine repressible $P3_{nmt1}$ promoter led to Wee1 hyperphosphorylation by both Cdr2(1–330) and Cdr2(1–590) (Fig. S3). For both Cdr2 truncation constructs, the catalytically inactive E177A mutant prevented hyperphosphorylation of Wee1 (Figs. 7*E* and S3). We conclude that hyperphosphorylation of Wee1 is not sufficient to induce premature mitotic entry when Cdr2 levels increase. This result emphasizes the functional importance of Wee1 sequestration in driving early mitosis. Put together, our results show that both kinase activity and clustering are required for elevated levels of Cdr2 to induce premature mitotic entry.

Discussion

We have shown that increased expression of Cdr2 causes early mitotic entry through a mechanism based on

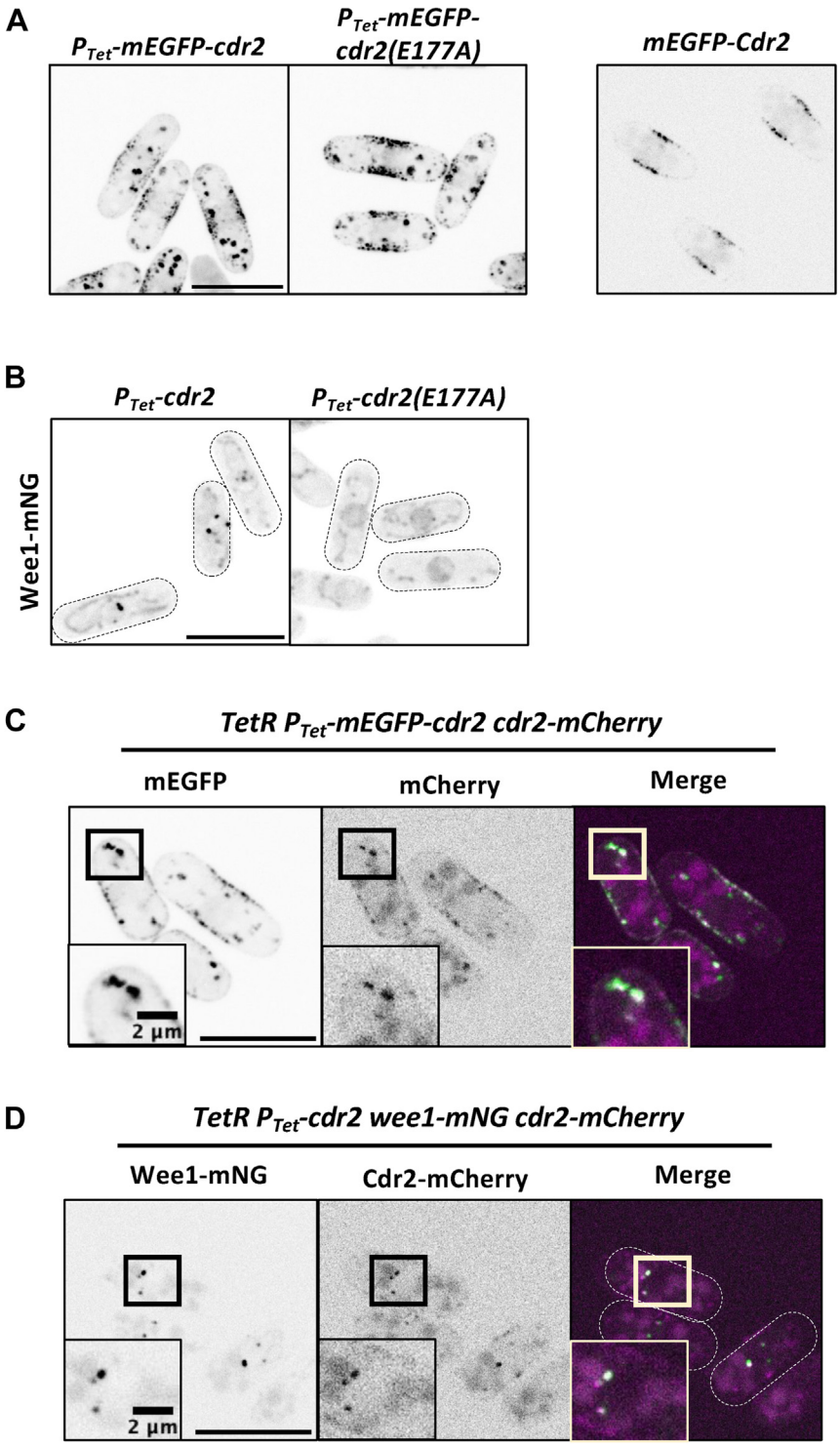

Figure 3. Cdr2 and Wee1 localize to cytoplasmic puncta in *P_{Tet}-cdr2*–induced conditions. *A*, *left*, images of the indicated strains after incubation with Tet for 6 h. *Right*, image of endogenously expressed mEGFP-Cdr2 for comparison. Maximum intensity projections of 0.5 µm-spaced focal planes covering 2 µm in cell middle. *B*, Wee1-mNG in the indicated strains after incubation with Tet for 6 h. Single focal plane. Cell boundaries are outlined. *C*, colocalization of P_{Tet}-mEGFP-Cdr2 and P_{cdr2}-Cdr2-mCherry after incubation with Tet for 6 h. Maximum intensity projections of 0.5 µm-spaced focal planes covering 1 µm in cell middle. *D*, colocalization of P_{cdr2}-Cdr2-mCherry and Wee1-mNG after Tet-induced expression of *P_{Tet}-cdr2*. Maximum intensity projections of 0.5 µm-spaced focal planes covering 1 µm in cell middle. All scale bars, 10 µm. *Boxed regions* are zoomed in *lower corner panels*. Single channel images are shown with inverted LUT. Tet, anhydrotetracycline.

hyperphosphorylation and sequestration of Wee1 (Fig. 8). This phenotype means that Cdr2 overexpression *versus* Cdr2 loss-of-function mutations have opposite effects: *cdr2Δ* mutants delay mitotic entry leading to enlarged cells, while *cdr2+* overexpression causes premature mitotic entry leading to small cells.

The mechanism that we have uncovered for upregulated Cdr2 expands current models for regulation of cell size

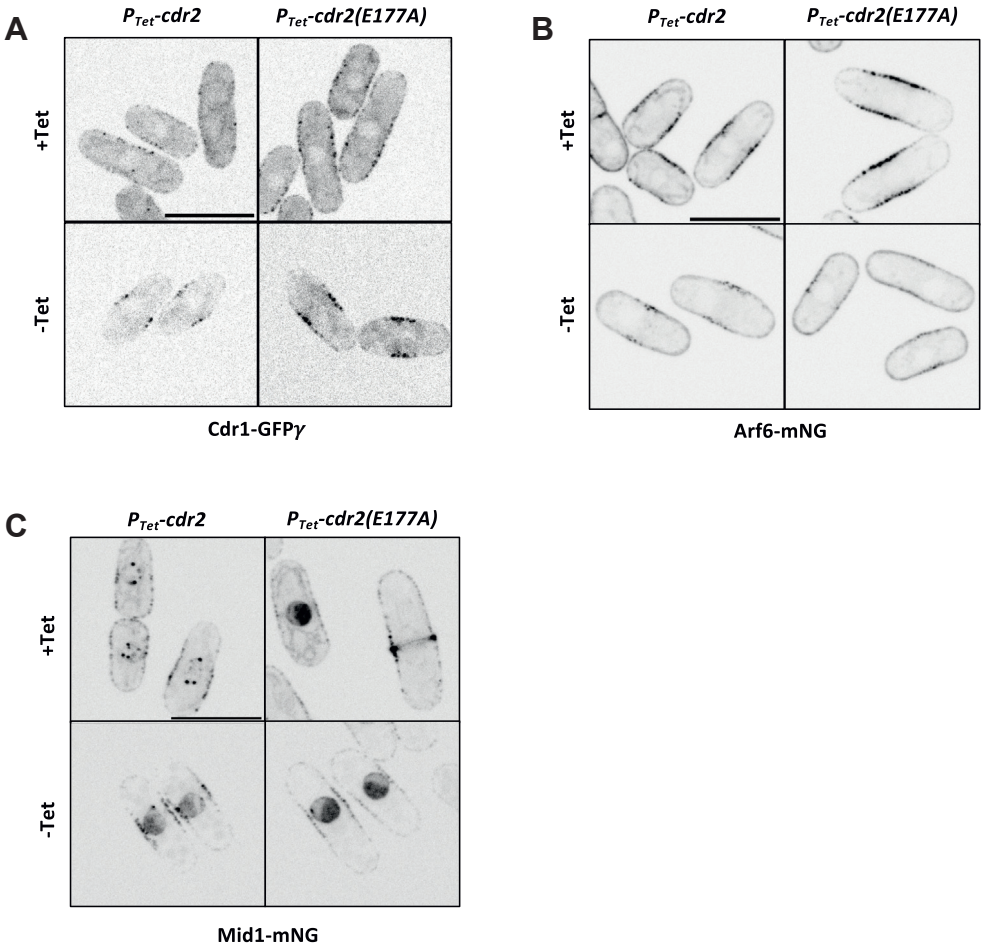

Figure 4. Characterization of Cdr2 clusters. *A*, localization of Cdr1-GFPγ before (*lower*) and after (*upper*) P_{Tet}-*cdr2* and P_{Tet}-*cdr2(E177A)* induction. *B*, Arf6-mNG imaged before and after P_{Tet}-*cdr2* and P_{Tet}-*cdr2(E177A)* induction. *C*, Mid1-mNG localization before and after induction of P_{Tet}-*cdr2* and P_{Tet}-*cdr2(E177A)*. Maximum intensity projections of 0.5 μm-spaced focal planes covering middle 1 μm of cells. Scale bars 10 μm.

through Wee1. At endogenous expression levels, Cdr2 forms nodes that bring together Cdr1 and Wee1 to stimulate inhibitory phosphorylation of Wee1. Past studies have focused on inhibitory phosphorylation of Wee1 by Cdr1 as the sole inhibitory mechanism in this system. However, such a model does not explain the stronger cell size defect of *cdr2Δ* mutant cells when compared to *cdr1Δ* cells. Our work with the tetracycline-regulated expression system shows that upregulated Cdr2 can sequester Wee1 away from the nucleus, leading to changes in cell size even in the absence of Cdr1. Concentration of Wee1 at these Cdr2 clusters likely prevents its interactions with Cdk1 in the nucleus. An important next step to understand this mechanism will be the identification and characterization of Cdr2-dependent phosphorylation sites on Wee1.

Based on our current findings, we propose that Cdr2 plays two roles in regulating cell size through Wee1. The first role is the previously described scaffolding mechanism to promote inhibitory phosphorylation of Wee1 by Cdr1, which leads to inhibition of Wee1 catalytic activity. This first role is dependent on Cdr1. The second role is to sequester Wee1 away from the nucleus, as demonstrated in our current study. This second role regulates the localization but not catalytic activity of Wee1 and is independent of Cdr1 as

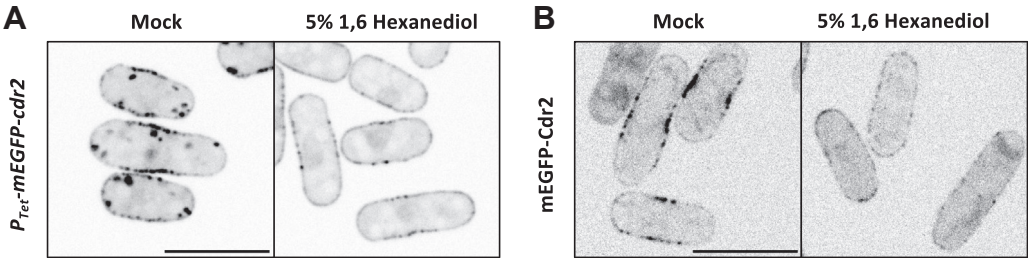

Figure 5. Cdr2 structures are disrupted by 1,6-hexanediol. *A*, induced P_{Tet}-*mEGFP-cdr2* cells were treated with 5% 1,6-hexanediol. *B*, treatment of endogenously expressed *mEGFP-cdr2* cells with 5% 1,6-hexanediol disrupts cortical nodes. Middle focal plane images; scale bar is 10 μm.

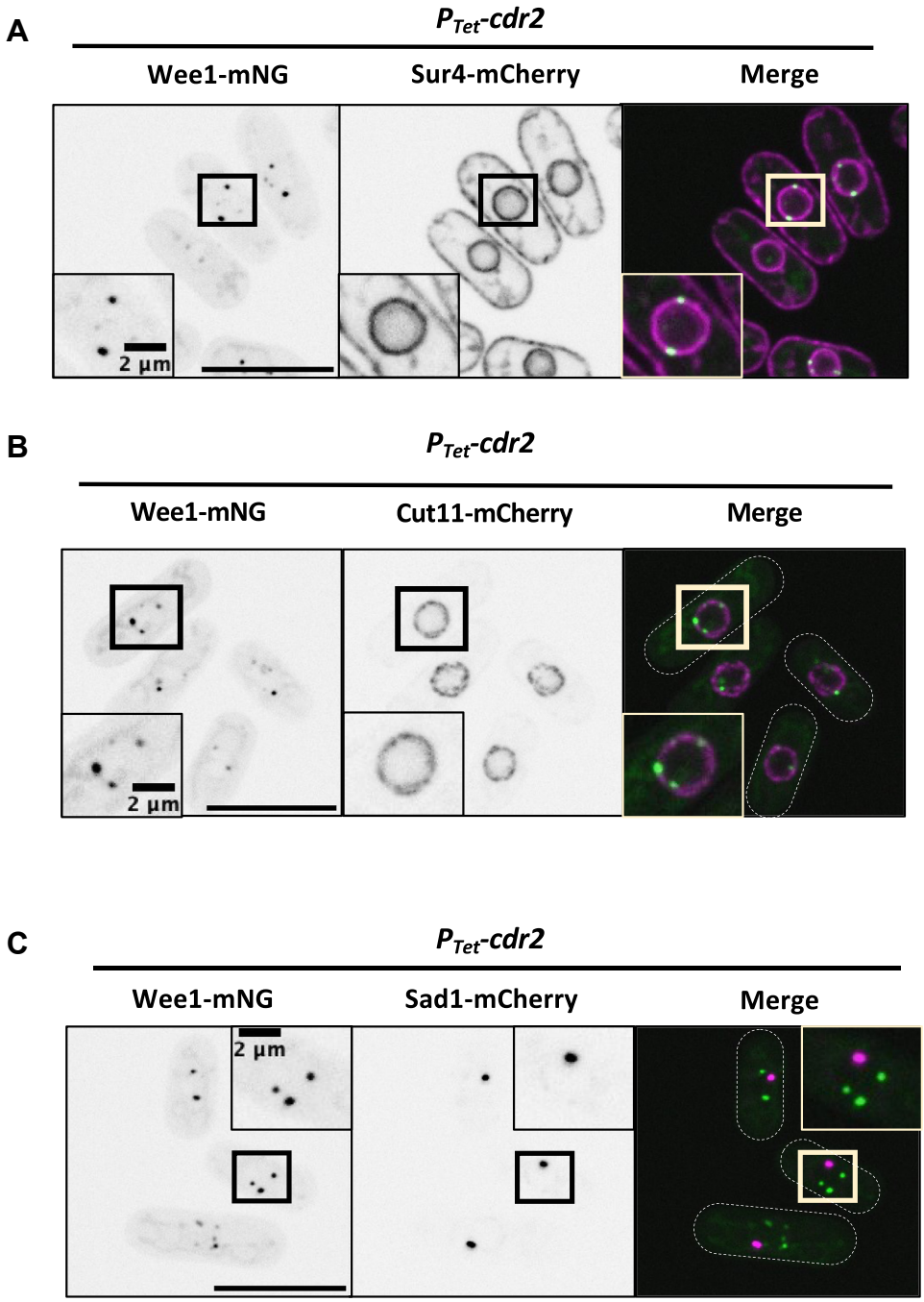

Figure 6. Localization of Wee1 puncta in P_{Tet}-*cdr2*. *A*, Wee1-mNG and Sur4-mCherry after P_{Tet}-*cdr2* induction. *B*, localization of Wee1-mNG and Cut11-mCherry after P_{Tet}-GST-Cdr2 induction. *C*, Wee1-mNG and Sad1-mCherry after P_{Tet}-*cdr2* induction. All scale bars are 10 µm. All images are maximum intensity projections from 0.5 µm-spaced focal planes spanning 1 µm in cell middle. Single channel images are shown with inverted LUT.

shown by our experiments in *cdr1Δ cdr2Δ* cells. This second role is supported by localization of Wee1 to endogenous Cdr2 cortical nodes in *cdr1Δ* cells (9). By identifying this Cdr1-independent mechanism for regulation of Wee1 and cell size by Cdr2, we show that the Cdr2-Cdr1-Wee1 pathway has two, interconnected mechanism that inhibit Wee1 for cell size control. Cdr1-independent regulation of Wee1 localization by Cdr2 also provides an explanation for the stronger cell size defect of *cdr2Δ* cells as compared to *cdr1Δ* cells.

Our results also have implications for signaling pathways beyond Cdr2 and fission yeast. Spatial sequestration has the capacity to turn signaling pathways on and off, particularly when transitioning between nuclear and cytoplasmic compartments. Our work demonstrates a role for sequestration of Wee1 away from its nuclear target Cdk1. Interestingly, Cdc25, the phosphatase that counteracts Wee1 activity on Cdk1, is also regulated by nuclear accumulation, and Cdc25 sequestration in the cytoplasm is a mechanism to delay entry into mitosis during DNA damage (27). Therefore, sequestration

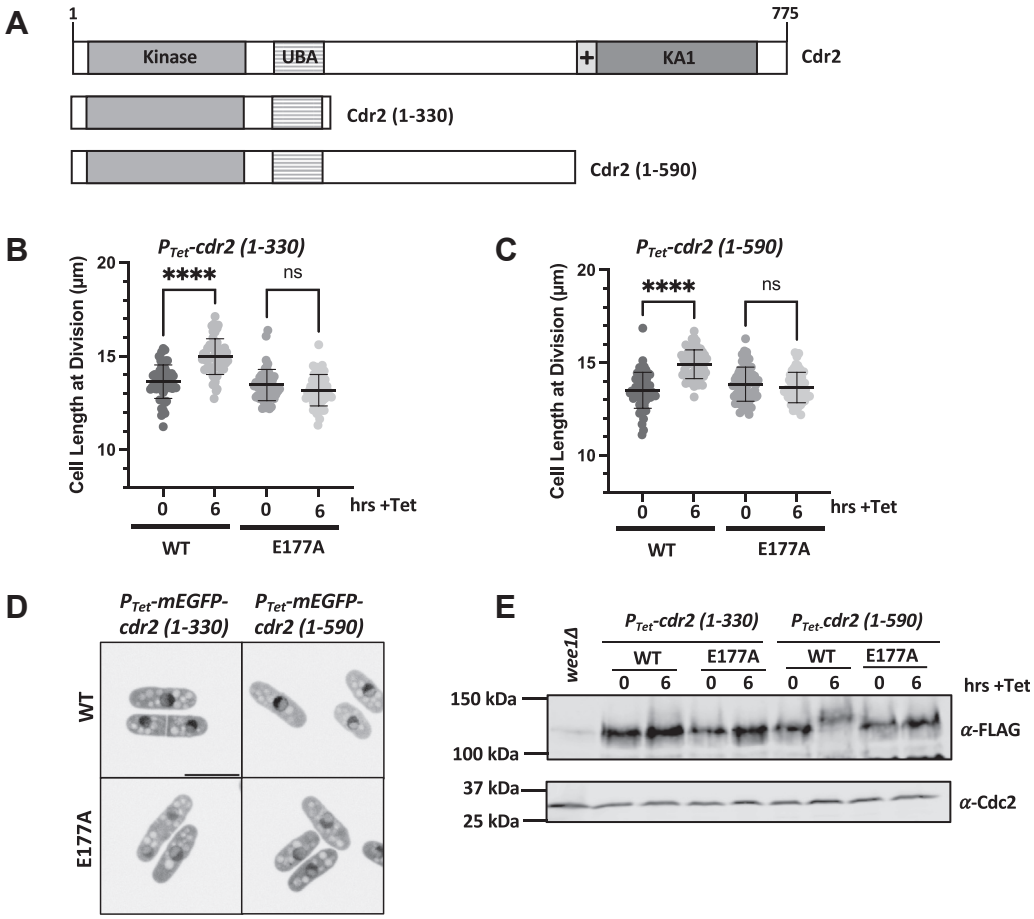

Figure 7. Analysis of Cdr2 truncation mutants. *A*, domain layout of Cdr2 constructs. *B*, cell size at division for wildtype and E177A mutant versions of P_{Tet}-*cdr2*(1–330). n ≥ 50 cells. *C*, cell size at division for wildtype and E177A mutant versions of P_{Tet}-*cdr2*(1–590). n ≥ 50 cells. ns, not significant ($p > 0.05$). ****$p <$ 0.0001 determined by ANOVA. *D*, localization of the indicated constructs after 6-h Tet incubation. Scale bar 10 µm. *E*, Western blot for Wee1-FLAG before and after induction of P_{Tet}-*mEGFP-cdr2* truncations. +, basic patch; KA1, Kinase associated-1; UBA, ubiquitin-associated.

away from the nucleus is a common regulatory mechanism for both the inhibitory kinase (Wee1) and the activating phosphatase (Cdc25) for Cdk1.

We have shown that sequestration of Wee1 in the cytoplasm can be driven by oligomeric clusters formed by Cdr2. A growing number of protein kinases function in oligomeric clusters that contribute to their activity and regulation. Examples from multiple animal cell polarity and receptor-associated tyrosine kinase systems have revealed that clustering can promote kinase signaling (37–39). Similarly, regulated clustering of bacterial kinases such as *C. crescentus* DivJ can activate downstream signals (40). Recent work has

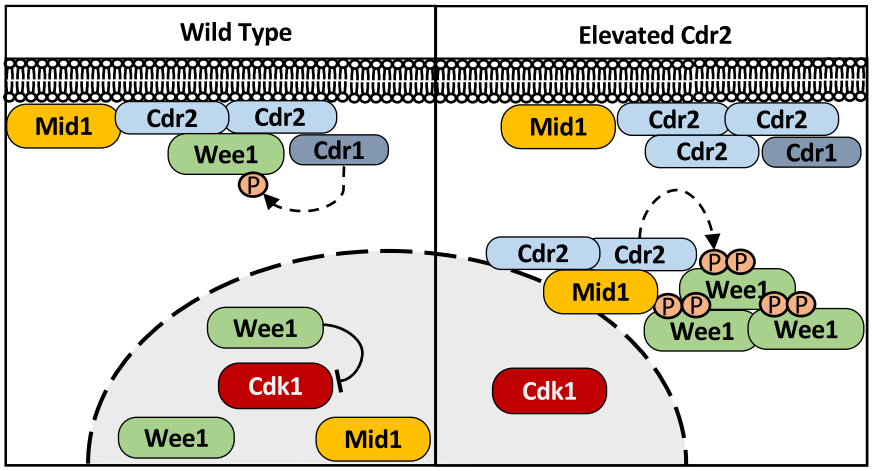

Figure 8. Working model for mechanism of Wee1 inhibition by overexpressed Cdr2.

identified aspects of condensed-phase signaling within multiprotein clusters that promote signal transduction in phosphorylation pathways (41). This widespread phenomenon makes kinase clustering an attractive candidate for synthetic biology approaches that seek to control signaling networks (42). In our system, we anticipate that Cdr2 itself is the direct binding ligand of Wee1 based on previous protein–protein interaction assays (9), which means that the clusters could directly recruit and sequester their target. Our work adds a new layer to this theme by showing how kinase clusters can sequester substrates to control downstream signaling, which could represent a new mechanism for these and other signaling systems.

Experimental procedures

Yeast strains and growth

Standard *S. pombe* media and methods were used (43). Strains in this study are listed in Table S1, and plasmids used are listed in Table S2. All P_{Tet} plasmids were generated using Gibson reactions (NEB HiFi Assembly Mix) from PCR products. These plasmids contain the strong *eno101* promoter with tet operons (28) A linearized version of this plasmid was generated by PCR and then transformed into strains containing TetR. Transformants were selected by hygromycin resistance and leucine auxotrophy. In Figures 3*B* and 6, cells were cultured in YE4S (rich) media overnight and then switched to EMM4S (minimal) media for at least 24 h prior to induction and imaging. All other imaging was performed in YE4S.

Overexpression of Cdr2

Strains confirmed for P_{Tet}-*GST-cdr2* were grown in YE4S at 32 C for cell size measurements and Western blot sample collection or alternatively at 25 C for live-cell fluorescent microscopy. With the exception of mEGFP-tagged constructs, all other P_{Tet}-*cdr2* constructs in our study contained an N-terminal GST tag that was used to verify expression by Western blot. Cells were maintained in logarithmic phase growth at least 24 h prior to induction. Overexpression was induced using a final concentration of 5 μg/ml Tet (Sigma), from a 10 mg/ml stock in DMSO (stored at −20 C). Uninduced cells in log phase were imaged for timepoint zero, and cells that were induced were seeded at A_{600} = 0.05 and left to grow in the presence of Tet for 6 h before imaging. For experiments with *wee1-50* strains, cells were treated with DMSO or Tet for 2 h at 25 C and then were left at 25 C or shifted to 36 C for the remaining 4 h. In Fig. S3, pREP3x overexpression of Cdr2, cells containing pREP3x-6His-Cdr2 plasmid were grown in EMM4S lacking leucine and containing thiamine at 32 C. Cultures were washed into media lacking thiamine to induce expression, and then samples were collected at the indicated times.

Western blots

To make whole cell lysates, two A_{600} units of cells were harvested at timepoint zero (prior to Tet addition) and at subsequent timepoints as indicated. Cells were pelleted, washed once with water, and pellets were flash frozen in liquid nitrogen. Samples were lysed by bead beating with Minibeadbeater-16 in SDS-PAGE sample buffer including protease and phosphatase inhibitors (15% glycerol, 4.5% SDS, 97.5 mM Tris pH6.8, 10% 2-mercaptoethanol, 50 mM β-glycerophosphate, 50 mM sodium fluoride, 5 mM sodium orthovanadate, 1× EDTA-free protease inhibitor cocktail (Sigma Aldrich)) and then incubated at 99 C for 5 min. Following brief centrifugation, clarified lysate was separated by SDS-PAGE and transferred to nitrocellulose using Trans-blot Turbo Transfer System (Bio-Rad). Proteins were probed with antibodies against FLAG M2 (Sigma), Cdc2 (Santa Cruz Biotechnologies SC-53217), and Wee1 (9). Blots were imaged on a LiCor Odyssey CLx.

For quantification in Figure 1*C*, three independently grown biological replicate cultures were prepared for each condition and analyzed from the presented Western blot. Samples were prepared in parallel as described above, and 10 μl of each sample was loaded per lane. Background-subtracted band intensities were measured with ImageStudioLite software. The average band intensity of the three endogenously expressed Cdr2-9gly-5xFLAG samples was set to 1. The bar graph shows each individual data point normalized to this average. The P_{Tet}-*cdr2-9Gly-5xFLAG* strain in this experiment was a second copy expressed in addition to with the untagged, endogenous Cdr2. Data were graphed using Prism9 GraphPad.

Lambda phosphatase

The protocol was adapted from previous work (44) using phosphatase buffer prepared to 1× and containing 1 mM $MnCl_2$. In brief: two A_{600} units of cells were pelleted, flash frozen in nitrogen, lysed by bead beating in 200 μl phosphatase buffer with glass beads for 1 min, placed on ice for 1 min, and then centrifuged at 15,000*g* for 1 min. For each reaction, 20 μl of this lysate was mixed with 800U lambda phosphatase (New England Biolabs) or untreated. These reactions were incubated for 30 min at 30 C. Reactions were stopped by addition of 2× SDS-PAGE sample buffer (30% glycerol, 9% SDS, 195 mM Tris pH 6.8, 15% 2-mercaptoethanol) and boiled for 5 min before analyzing by SDS-PAGE as described above.

Widefield microscopy

Images for cell length measurements (Figs. 2 and 7, *B* and *C*) were captured at room temperature on a DeltaVision imaging system comprised of an Olympus IX-71 inverted wide-field microscope, a Photometrics Cool-SNAP HQ2 camera, an Insight solid-state illumination unit, and a 1.42 NA Plan Apo 60× oil objective. Cells were grown as specified above and imaged after addition of Blankophor cell wall stain to identify dividing, septated cells.

Spinning-disc confocal microscopy

Fluorescent live-cell microscopy (Figs. 3–6, 7*D*, and S2) was performed at room temperature on a Yokogawa CSU-WI imaging system, which was equipped with a Nikon Eclipse Ti2 inverted microscope, a 100 × 1.45 NA CFI Plan

Apochromat Lambda objective lens (Nikon); 405-, 488-, and 561-nm laser lines; and a photometrics Prime BSI camera. Due to fluorescence of Tet, imaging of fluorescently tagged proteins was performed on cells that had been washed into fresh Tet-free media for 20 min prior to imaging. 1,6-hexanediol-treated cells were also imaged on this system (Fig. 5). These cells were grown and induced with Tet in YE4S as described, washed for 20 min into fresh YE4S, then incubated another 10 min in the presence or absence of 5% (w/v) 1,6-hexanediol dissolved in media.

Cell length measurements and statistics

Cell length measurements were made using Line Tool in FIJI Image J (45) on images of cells stained with the cell wall dye Blankophor. The resulting data were graphed and statistically analyzed in Prism9 GraphPad. Cell length measurements in Figure 2*E* were compared by Welch's *t* test. All other cell length measurements were compared by one-way ANOVA followed by Tukey's multiple comparison test, which compares each mean within an experiment to each other.

Data availability

All data are contained within the manuscript.

Supporting information—This article contains supporting information.

Acknowledgments—We thank members of the Moseley laboratory for helpful discussions and comments on the manuscript. We thank the Nurse laboratory for sharing P_{Tet} strains and plasmids, Scott Curran for experimental advice, and the Biomolecular Targeting Core (bioMT) for equipment (P20-GM113132).

Author contributions—R. A. B. and J. B. M. conceptualization; R. A. B. and J. B. M. methodology; R. A. B. formal analysis; R. A. B. investigation; R. A. B. and J. B. M. writing–original draft; R. A. B. and J. B. M. writing–review & editing; J. B. M. supervision; J. B. M. project administration; J. B. M. funding acquisition.

Funding and additional information—This work was supported by grants from the National Institute of General Medical Sciences (R01GM099774 and R01GM133856) to J. B. M.

Conflict of interest—The authors declare that they have no conflicts of interest with the contents of this article.

Abbreviations—The abbreviations used are: KA1, Kinase associated-1; Tet, anhydrotetracycline; UBA, ubiquitin-associated.

References

1. Morgan, D. O. (1997) Cyclin-dependent kinases: engines, clocks, and microprocessors. *Annu. Rev. Cell Dev. Biol.* **13**, 261–291
2. Wieser, S., and Pines, J. (2015) The biochemistry of mitosis. *Cold Spring Harb. Perspect. Biol.* **7**, a015776
3. Coleman, T. R., and Dunphy, W. G. (1994) Cdc2 regulatory factors. *Curr. Opin. Cell Biol.* **6**, 877–882
4. Kellogg, D. R. (2003) Wee1-dependent mechanisms required for coordination of cell growth and cell division. *J. Cell Sci.* **116**, 4883–4890
5. Millar, J. B., and Russell, P. (1992) The cdc25 M-phase inducer: an unconventional protein phosphatase. *Cell* **68**, 407–410
6. Rupes, I. (2002) Checking cell size in yeast. *Trends Genet.* **18**, 479–485
7. Russell, P., and Nurse, P. (1987) Negative regulation of mitosis by wee1+, a gene encoding a protein kinase homolog. *Cell* **49**, 559–567
8. Russell, P., and Nurse, P. (1986) cdc25+ functions as an inducer in the mitotic control of fission yeast. *Cell* **45**, 145–153
9. Allard, C. A. H., Opalko, H. E., Liu, K.-W., Medoh, U., and Moseley, J. B. (2018) Cell size-dependent regulation of Wee1 localization by Cdr2 cortical nodes. *J. Cell Biol.* **217**, 1589–1599
10. Coleman, T. R., Tang, Z., and Dunphy, W. G. (1993) Negative regulation of the wee1 protein kinase by direct action of the nim1/cdr1 mitotic inducer. *Cell* **72**, 919–929
11. Parker, L. L., Walter, S. A., Young, P. G., and Piwnica-Worms, H. (1993) Phosphorylation and inactivation of the mitotic inhibitor Wee1 by the nim1/cdr1 kinase. *Nature* **363**, 736–738
12. Wu, L., and Russell, P. (1993) Nim1 kinase promotes mitosis by inactivating Wee1 tyrosine kinase. *Nature* **363**, 738–741
13. Opalko, H. E., Nasa, I., Kettenbach, A. N., and Moseley, J. B. (2019) A mechanism for how Cdr1/Nim1 kinase promotes mitotic entry by inhibiting Wee1. *Mol. Biol. Cell* **30**, 3015–3023
14. Russell, P., and Nurse, P. (1987) The mitotic inducer nim1+ functions in a regulatory network of protein kinase homologs controlling the initiation of mitosis. *Cell* **49**, 569–576
15. Kanoh, J., and Russell, P. (1998) The protein kinase Cdr2, related to Nim1/Cdr1 mitotic inducer, regulates the onset of mitosis in fission yeast. *Mol. Biol. Cell* **9**, 3321–3334
16. Morrell, J. L., Nichols, C. B., and Gould, K. L. (2004) The GIN4 family kinase, Cdr2p, acts independently of septins in fission yeast. *J. Cell Sci.* **117**, 5293–5302
17. Martin, S. G., and Berthelot-Grosjean, M. (2009) Polar gradients of the DYRK-family kinase Pom1 couple cell length with the cell cycle. *Nature* **459**, 852–856
18. Moseley, J. B., Mayeux, A., Paoletti, A., and Nurse, P. (2009) A spatial gradient coordinates cell size and mitotic entry in fission yeast. *Nature* **459**, 857–860
19. Young, P. G., and Fantes, P. A. (1987) Schizosaccharomyces pombe mutants affected in their division response to starvation. *J. Cell Sci.* **88**, 295–304
20. Breeding, C. S., Hudson, J., Balasubramanian, M. K., Hemmingsen, S. M., Young, P. G., and Gould, K. L. (1998) The cdr2(+) gene encodes a regulator of G2/M progression and cytokinesis in Schizosaccharomyces pombe. *Mol. Biol. Cell* **9**, 3399–3415
21. Bhatia, P., Hachet, O., Hersch, M., Rincon, S. A., Berthelot-Grosjean, M., Dalessi, S., *et al.* (2014) Distinct levels in Pom1 gradients limit Cdr2 activity and localization to time and position division. *Cell Cycle* **13**, 538–552
22. Pan, K. Z., Saunders, T. E., Flor-Parra, I., Howard, M., and Chang, F. (2014) Cortical regulation of cell size by a sizer cdr2p. *Elife* **3**, e02040
23. O'Neill, E. M., Kaffman, A., Jolly, E. R., and O'Shea, E. K. (1996) Regulation of PHO4 nuclear localization by the PHO80-PHO85 cyclin-CDK complex. *Science* **271**, 209–212
24. Komeili, A., and O'Shea, E. K. (1999) Roles of phosphorylation sites in regulating activity of the transcription factor Pho4. *Science* **284**, 977–980
25. Wong, W., and Scott, J. D. (2004) AKAP signalling complexes: focal points in space and time. *Nat. Rev. Mol. Cell Biol.* **5**, 959–970
26. Reiser, V., Ammerer, G., and Ruis, H. (1999) Nucleocytoplasmic traffic of MAP kinases. *Gene Expr.* **7**, 247–254
27. Lopez-Girona, A., Furnari, B., Mondesert, O., and Russell, P. (1999) Nuclear localization of Cdc25 is regulated by DNA damage and a 14-3-3 protein. *Nature* **397**, 172–175

28. Patterson, J. O., Rees, P., and Nurse, P. (2019) Noisy cell-size-correlated expression of cyclin B drives probabilistic cell-size homeostasis in fission yeast. *Curr. Biol.* **29**, 1379–1386.e4
29. Opalko, H. E., Miller, K. E., Kim, H.-S., Vargas-Garcia, C. A., Singh, A., Keogh, M.-C., *et al.* (2022) Arf6 anchors Cdr2 nodes at the cell cortex to control cell size at division. *J. Cell Biol.* **221**, e202109152
30. Almonacid, M., Moseley, J. B., Janvore, J., Mayeux, A., Fraisier, V., Nurse, P., *et al.* (2009) Spatial control of cytokinesis by Cdr2 kinase and Mid1/anillin nuclear export. *Curr. Biol.* **19**, 961–966
31. Patel, S. S., Belmont, B. J., Sante, J. M., and Rexach, M. F. (2007) Natively unfolded nucleoporins gate protein diffusion across the nuclear pore complex. *Cell* **129**, 83–96
32. Ribbeck, K., and Görlich, D. (2002) The permeability barrier of nuclear pore complexes appears to operate via hydrophobic exclusion. *EMBO J.* **21**, 2664–2671
33. Alberti, S., Gladfelter, A., and Mittag, T. (2019) Considerations and challenges in studying liquid-liquid phase separation and biomolecular condensates. *Cell* **176**, 419–434
34. Düster, R., Kaltheuner, I. H., Schmitz, M., and Geyer, M. (2021) 1,6-Hexanediol, commonly used to dissolve liquid-liquid phase separated condensates, directly impairs kinase and phosphatase activities. *J. Biol. Chem.* **296**, 100260
35. Guzmán-Vendrell, M., Rincon, S. A., Dingli, F., Loew, D., and Paoletti, A. (2015) Molecular control of the Wee1 regulatory pathway by the SAD kinase Cdr2. *J. Cell Sci.* **128**, 2842–2853
36. Rincon, S. A., Bhatia, P., Bicho, C., Guzman-Vendrell, M., Fraisier, V., Borek, W. E., *et al.* (2014) Pom1 regulates the assembly of Cdr2-Mid1 cortical nodes for robust spatial control of cytokinesis. *J. Cell Biol.* **206**, 61–77
37. Douglass, A. D., and Vale, R. D. (2005) Single-molecule microscopy reveals plasma membrane microdomains created by protein-protein networks that exclude or trap signaling molecules in T cells. *Cell* **121**, 937–950
38. Dickinson, D. J., Schwager, F., Pintard, L., Gotta, M., and Goldstein, B. (2017) A single-cell biochemistry approach reveals PAR complex dynamics during cell polarization. *Dev. Cell* **42**, 416–434.e11
39. Mayer, B. J., and Yu, J. (2018) Protein clusters in phosphotyrosine signal transduction. *J. Mol. Biol.* **430**, 4547–4556
40. Saurabh, S., Chong, T. N., Bayas, C., Dahlberg, P. D., Cartwright, H. N., Moerner, W. E., *et al.* (2022) ATP-responsive biomolecular condensates tune bacterial kinase signaling. *Sci. Adv.* **8**, eabm6570
41. Sang, D., Shu, T., Pantoja, C. F., Ibáñez de Opakua, A., Zweckstetter, M., and Holt, L. J. (2022) Condensed-phase signaling can expand kinase specificity and respond to macromolecular crowding. *Mol. Cell* **82**, 3693–3711.e10
42. Yoshikawa, M., Yoshii, T., Ikuta, M., and Tsukiji, S. (2021) Synthetic protein condensates that inducibly recruit and release protein activity in living cells. *J. Am. Chem. Soc.* **143**, 6434–6446
43. Moreno, S., Klar, A., and Nurse, P. (1991) Molecular genetic analysis of fission yeast Schizosaccharomyces pombe. *Methods Enzymol.* **194**, 795–823
44. Lucena, R., Alcaide-Gavilán, M., Anastasia, S. D., and Kellogg, D. R. (2017) Wee1 and Cdc25 are controlled by conserved PP2A-dependent mechanisms in fission yeast. *Cell Cycle* **16**, 428–435
45. Schindelin, J., Arganda-Carreras, I., Frise, E., Kaynig, V., Longair, M., Pietzsch, T., *et al.* (2012) Fiji: an open-source platform for biological-image analysis. *Nat. Methods* **9**, 676–682